Biosensors and Bioelectronics 24 (2009) 1462–1468

Contents lists available at ScienceDirect

Biosensors and Bioelectronics

journal homepage: www.elsevier.com/locate/bios

A novel design of multifunctional integrated cell-based biosensors for simultaneously detecting cell acidification and extracellular potential

Hui Yu[a,b], Hua Cai[a], Wei Zhang[a], Lidan Xiao[a], Qingjun Liu[a], Ping Wang[a,b,*]

[a] Biosensor National Special Laboratory, Key Laboratory of Biomedical Engineering of Ministry of Education, Department of Biomedical Engineering, Zhejiang University, Hangzhou 310027, PR China
[b] State Key Laboratory of Transducer Technology, Chinese Academy of Sciences, 200050, PR China

ARTICLE INFO

Article history:
Received 14 April 2008
Received in revised form 26 August 2008
Accepted 28 August 2008
Available online 6 September 2008

Keywords:
Cell-based biosensors
Acidification
Extracellular potential
LAPS array
Parallel detection

ABSTRACT

The paper discussed a novel design of multifunctional cell-based biosensors for simultaneously detecting cell acidification and extracellular potential. Employing living cells such as cardiac myocytes as a source for the light addressable potentiometric sensor (LAPS) array, this cell-based biosensor was able to monitor both the acidification and extracellular potential in parallel. For LAPS array fabrication, part of the silicon base was heavily doped with boron to form separate testing areas. Detecting system was built involving lock-in amplifier and digital demodulation with FFT methods. This LAPS array showed a good sensitivity of 53.9 mV/pH to H^+ with good linearity. Each testing area for extracellular potential detection was decreased to 200 μm × 200 μm in size to obtain a better sensitivity. Experiment results showed that this LAPS array could monitor the acidification of cells as well as the extracellular potential with good sensitivity. This novel integrated biosensor will be useful for multi-parameter extracellular monitoring and can possibly be a platform for drug screening.

1. Introduction

In a living cell, thousands of biological reactions happen which are more or less coupled to each other and represent a complicated network. It is a different approach in functional online analysis of living cells in physiologically controlled environments for extended periods of time. A rigorous preselection of identified compounds by in vitro cellular screening is necessary prior to using the drug candidates for the further time consuming and expensive stage, e.g. in animal models. So nowadays, the aim is focused on integration of different microelectronic sensors into miniaturized biochips for a multifunctional online analysis of living cells.

Cell acidification and extracellular potential signals such as action potential are important parameters showing cell's status. Acidification plays an important role in cell metabolism. Usually, the extracellular pH change is used to indicate the living condition of cells. For extracellular detection of cell metabolic substances, light addressable potentiometric sensor (LAPS) has many advantages, such as high sensitivity, easy encapsulation, and perfect to make a microchamber for cell experiments. Many attempts have been made to commercialize the LAPS system (Adami et al., 1995; Wolf et al., 1998). One successfully commercialized system using the LAPS for determination of the extracellular acidification of living cells is the Cytosensor Microphysiometer system, released in 1990 by Molecular Devices Corp. (Sunnyvale, CA).

To detect intracellular potentials, traditional glass pipettes with electrodes that put surround or in cells with the help of patch clamp will meet some problems such as high requirements in rigidity, diameters and impedance of electrodes. Besides, long-time detections cannot be performed since it is harmful to the cell (Hamill et al., 1981). Extracellular potential is usually measured employing field-effect transistor arrays (FET) (Sprössler et al., 1999) or substrate-integrated microelectrode arrays (MEA) (Connolly et al., 1990; Denyer et al., 1998). However, these two techniques both suffer from geometrical restriction and measurements are limited to a fix number of recording sites. LAPS is a surface potential detector with spatial resolution, based on silicon technology (Hafeman et al., 1988). With cells cultured on the surface of LAPS, extracellular potential can also be monitored (Xu et al., 2005). Comparing to MEA and FET, any desirable detection site can be freely selected by moving the light pointer across the surface of LAPS. Therefore, surface potential measurements are no longer restricted to predetermined sites.

The monitoring efficiency of extracellular parameters can be greatly improved by high throughput screening platforms. Due

* Corresponding author at: Biosensor National Special Laboratory, Key Laboratory of Biomedical Engineering of Ministry of Education, Department of Biomedical Engineering, Zhejiang University, Hangzhou 310027, PR China. Tel.: +86 571 87952832; fax: +86 571 87951676.
E-mail address: cnpwang@zju.edu.cn (P. Wang).

0956-5663/$ – see front matter © 2008 Elsevier B.V. All rights reserved.
doi:10.1016/j.bios.2008.08.045

to the spatial resolving power, LAPS has an advantage for multi-sensing application (Shimizu et al., 1994). Usually, when used for multi-sensing, LAPS can detect several different ions' concentration in parallel (Men et al., 2005; Wang et al., 2005). However, when these LAPS array were used for cell analysis, only chemical signals but no potential signals were monitored. Chemical signals and potential signals of cells show great connections. Thus, it will be helpful for cell analysis if both kinds of information can be obtained.

In this work, we discussed a multifunctional cell-based biosensor, which can determine cell acidification and monitor the extracellular potential signals simultaneously. Fabrication of LAPS array as well as the detecting system was introduced. Cell experiments were presented to show the characteristics of the sensor and corresponding results were discussed in details.

2. Theory and sensor design

2.1. Light addressable potentiometric sensor (LAPS)

Light addressable potentiometric sensor with an electrolyte-insulation-semiconductor (EIS) structure is schematically shown in Fig. 1(a). Applying a dc bias voltage to the EIS structure, a depletion layer appears at the insulator (SiO_2)–semiconductor (Si) interface. Illuminating part of the surface with a modulated light induces a localized photo-induced current to be measured as a sensor signal, the amplitude of which depends on the local surface potential.

Characteristic *I–V* curve of n-type LAPS shows the relationship between the induced photocurrent and the bias voltage applied to the sensor chip (Fig. 1(b)). The regions of these sigmoid curves can be identified as follow. In the cut off region, there is no photocurrent. In the working region, the photocurrent rises almost linearly with decreasing voltage. The bias voltage is set to the point of the inflection of this curve and kept constant during the detection process. At this point the photocurrent is most sensitive to change in the surface potential. In the saturated region, the photocurrent is saturated, which means change of bias voltage within this range will not cause any change in photocurrent. Since the photocurrent changes with the bias voltage, if the bias voltage applied is kept constant, external potential changes coupled to the bias voltage can be determined by detecting the change of photocurrent.

For pH detection, a layer of Si_3N_4 is fabricated on the surface of LAPS. According to the site-binding theory (Siu and Cobbold, 1979; Bousse, 1982), a potential difference which is related to the concentration of H^+ in the electrolyte forms on the insulator (Si_3N_4/SiO_2)-solution interface. This potential is coupled to the bias voltage applied to the sensor. Larger concentration of H^+ provides a larger value of this potential difference, causing the *I–V* curve to shift along the negative half axis of bias voltage (Fig. 1(b)). When the bias voltage is kept constant in the middle region, change of the photocurrent indicates the pH change of the electrolyte.

LAPS is a surface potential detector with spatial resolution. Light pointer used for LAPS detection can be focused by microscope and optical lens, which suggests the LAPS possible for any desirable cell analysis. However, LAPS chip cannot be optimized to improve the spatial resolution substantially to the size of a single living cell (Parak et al., 1997), most likely to be between 30 and 100 μm, which means small cluster of cells or individual isolated cell can be chosen as the detecting object. After cells are cultured on the LAPS, a focused laser, 10 μm in diameter, is used to illuminate the front side of the chip to address the cells to be monitored. Excitable cells such as cardiac myocytes or neuron cells can generate extracellular action potential. This potential is coupled to the bias voltage applied to the LAPS, which correspondingly changes the amplitude of the photocurrent. Thus, by monitoring the photocurrent at a constant bias voltage, extracellular potential signals can be detected (Xu et al., 2005).

2.2. LAPS array

Illuminating different sensing areas with modulated lights of different frequencies generates a photocurrent signal, from which corresponding information of each testing site can be obtained by fast Fourier transform (FFT) methods (Cai et al., 2007). Comparing with conventional surface potential detectors such as FET or MEA, integration of LAPS array has many advantages. The most important feature of LAPS array is the great reduction of the required leads. For MEA, the number of required leads is the same as the number of electrodes, while for LAPS array, only one lead is necessary, regardless of the number of testing sites, which is important for high level integration (George et al., 2000). Besides, LAPS can detect extracellular potential as well as ion concentrations (Wu et

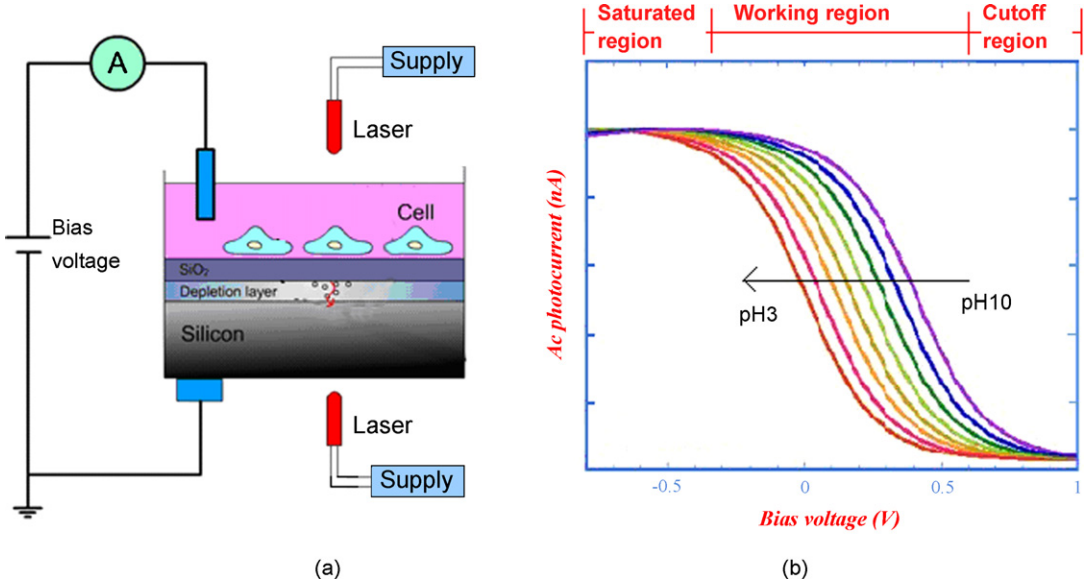

Fig. 1. Principle of the cell sensors based on LAPS. (a) The scheme of the LAPS. (b) Typical *I–V* curves of n-type LAPS.

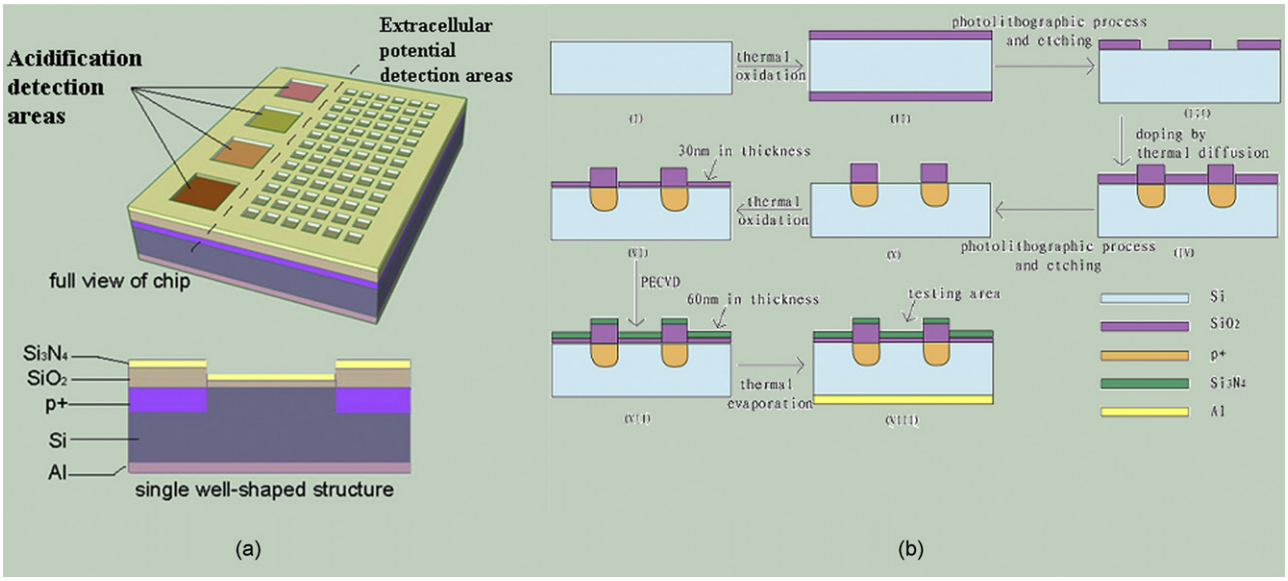

Fig. 2. (a) Schematic diagram of LAPS array sensor structure: the upper one is the full view of chip; the lower one is the well shaped structure of single testing area. (b) Fabrication process of the LAPS array.

al., 2001), which makes it suitable for multifunctional integration. Sensing surface of LAPS is extremely flat and free of metal contact. Thus it is easy for encapsulation of LAPS array and fabrication of micro testing chamber.

Since only a little part of the LAPS surface is illuminated with the modulated light pointer, unilluminated parts, where no photocurrent flows, act as stray capacitance and cause noises. Therefore, the smaller the total capacitance of the device is, the better the potential sensitivity will be. Small effective areas as well as a thick insulating layer reduce the total capacitance, and thus improve the potential sensitivity. Nevertheless, by reducing the effective LAPS surface to small areas, the advantage of the LAPS against surface potential detectors with discrete active sites is lost (George et al., 2000). According to our experience in cell experiments, we found it suitable at about 200 μm × 200 μm, both for cell culture and the noise level (Xu et al., 2006).

The integrated LAPS array sensor structure is schematically shown in Fig. 2(a). The chip has a total area of about 1 cm × 2 cm. Testing areas of two different sizes are fabricated on the same silicon chip by heavily doping the silicon between the testing areas. For extracellular potential signal detection, about 400 small square wells were fabricated in size of 200 μm × 200 μm and the plateau between two adjacent testing areas was 100 μm in width. Cells were cultured on the areas with small wells for potential detection. The depth of the well shaped structure was about several hundred nanometers, and we found that cells are more likely to grow on the testing areas of the arrays, which had lower altitude. Four larger wells for detection of cell acidification were 3 mm × 3 mm in size and 1 mm away from each other.

The fabrication process was easy and compatible with standard microelectronics facilities, shown in Fig. 2(b). A p-type silicon wafer (thickness of 450 μm) with ⟨1 0 0⟩ crystal orientation was used. First, a thick layer of silicon oxide was thermally grown on the surface. Then, after the pattern was transferred to the surface using photolithography, all silicon oxide, except that grown on testing areas (acting as a protector of substrate at testing areas from being doped in the following step), was removed by etching. Thermal diffusion doping was then carried out. As the silicon wafer is p-type, boron was selected as the impurity. There were two steps in doping process. First, a glass layer containing boron was pre-deposited on the sensing surface. Then pre-diffusion doped the surface of silicon to a small depth. After pre-diffusion, the glass layer was removed, followed by the redistribution step. During the redistribution step, a thick layer of silicon oxide about several hundred nanometers formed on the surface of doped areas, which participated in forming a well shaped structure. The doped part of the semiconductor was several micrometers in depth to cut off the depletion layer of adjacent detection sites. After the doping procedure, silicon oxide layer on testing areas was removed. Instead, a thin layer of silicon oxide, 30 nm in thickness, was thermally grown on testing sites and then a 60 nm silicon nitride layer as the sensitive layer to H^+ was deposited on the sensor chip by PECVD. At last, a thin layer of aluminum (thickness of 200 nm) was evaporated on the backside of the silicon chip to form an ohm contact.

After the sensor fabrication, following treatments were carried out respectively to the different functional areas. The sensing surface is free of metal contact and only two electrodes were required, hence encapsulation of the sensor is simple and less critical. The culture dish was sealed with a screwed cover coupled with inlet and outlet channels. The volume of culture medium or drugs can be controlled to about 100 μl each time.

2.3. Detecting system of LAPS array

A laser light with the wavelength at 690 nm (red) was used for illumination of extracellular potential detection. The laser was modulated at 10 kHz by the lock-in amplifier (SR830, Stanford Research System), and the power is about 0.2 mW. The laser was focused to about 10 μm in diameter through an optimized microscope so that it can be used to address a cluster of cells on the sensor chip. Four LEDs with the wavelength at 625 nm (red) were respectively driven at four different frequencies of crime numbers to avoid harmonic interference with a power of 50 mW. These LEDs illuminated the relative four testing areas for acidification detection. These five lights illuminated the sensor chip at the same time. A photocurrent signal including signals at all these five different frequencies was generated, respectively representing information of the five different testing sites. The detecting system was designed to sample the overall signal and extract signals at the five different frequencies.

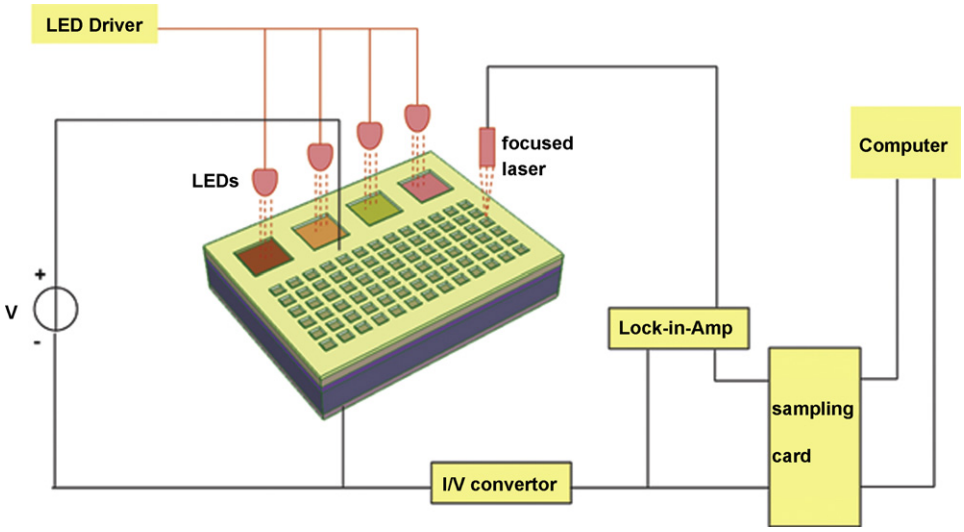

Fig. 3. The block diagram for LAPS array sensor detection.

Basically, single spike of action potential recorded lasts only several hundred milliseconds or even less (Sprössler et al., 1999, 1998; Fromherz, 2002). Thus, the sampling frequency should be high enough not to miss any action potential signals. Besides, for real-time monitoring of extracellular potential signals, time delay between sensing and display was preferred to be as small as possible. It is a different situation for acidification detection. Usually, the extracellular pH change is a long-time effect. Accumulation of H^+ in extracellular environment will not cause significant signals until several minutes (Hafner, 2000). Thus, for acidification detection, time delay between sampling and display was less critical. Usually, there were several seconds interval between two times of sampling.

The block diagram for LAPS array sensor detection is shown in Fig. 3.

A potentiostat (Model 273A, EG&G) was used to apply the bias voltage to the sensor chip and perform the *I–V*-converting. Due to the different requirements in the time delay, two different methods were combined for signal recording. For extracellular potential detection, after the overall photocurrent signal was *I–V* converted, the lock-in amplifier was used. As the laser was modulated at 10 kHz by the internal reference signals of the lock-in amplifier, the output of the lock-in amplifier was also the component at 10 kHz. Thus, only the signal generated at the testing site illuminated by the focused laser was preserved and demodulated, which indicated the extracellular potential signal. High sampling frequency up to 100 kHz was set to monitor the action potential. The lock-in amplifier can perform a fast demodulation of signals, and thus little delay was introduced for real-time monitoring.

For acidification detection, after the overall photocurrent signal of five different frequencies was converted to a potential signal, it was directly sampled to the computer for analysis. Signals generated at the four different sensing areas were gained separately by digitally demodulating the signal by software with FFT methods (Cai et al., 2007) at respective illuminating frequencies of the four LEDs, which were four different crime numbers. The overall signal was also sampled at 100 kHz. Data of 1 s were sampled every 5 s. Thus, there were 4 s for the software to perform digital demodulation of the signals at these four different frequencies and then display each part.

For a convenient handling, the cells are usually grown on sensor chips attached to small cell culture dish. The surface was coated with 100 μg/ml poly-L-ornithine, PBS and 8 μg/ml laminin (Ismail et al., 2003) prior to seeding cells on top of it. Cells on the chip were grown in DMEM-medium (D-5648, Sigma–Aldrich) supplemented with 7.6 mM HEPES and 30 mM $NaHCO_3$ at pH 7.4. Finally, the prepared cardiac myocytes were plated into the chamber of LAPS at densities of 1×10^5 cells/cm^2, at 37 °C under standard conditions of humidified air with 5% CO_2. Measurements were performed about 48 h after seeding the cells. For measurements the cell culture medium was substituted with electrolytic solution (125 mM NaCl, 1 mM KCl, 1 mM $MgCl_2$, 10 mM glucose and 20 mM HEPES at pH 7.4).

3. Results and discussion

3.1. Characteristics of LAPS array

I–V curves with illumination by the laser at both the testing area and the doped area were obtained. With illumination at the doped area, photocurrent was only about 1 nA, while with illumination at the testing area, good shaped *I–V* curve was obtained with about 2.5 uA in the saturated region. That is reasonable because of the far smaller resistance of the doped area than the substrate, very small potential drop will appear across the doped layer. Very small depletion layer exists in the doped area and thus induces such small photocurrent signals.

Noises of both LAPS array and single LAPS sensor with the same total areas were recorded. For the same total area of 1 cm × 2 cm, noise of the LAPS array was obviously smaller than noise of LAPS without array (6.205 ± 1.021 nA). Besides, the noise of small wells of 200 μm × 200 μm (2.166 ± 0.384 nA) was smaller than that of 3 mm × 3 mm (3.510 ± 0.829 nA). This is reasonable due to the high carrier concentration in the doped layer. Carriers from outside of the detection area are most likely to be recombined in the doped area. Depletion layers of testing areas are cut off from each other by the doped area, thus noises caused by charge carriers outside are minimized. Besides, the oxidation layer is thicker than that on the testing area, and thus decreases the total capacitance of the sensor as a contribution to a better potential sensitivity. Therefore, the testing sites on the LAPS array chip are acting exactly as individual LAPS

sensors with small effective areas, resulting in an improvement in potential sensitivity.

3.2. Acidification detection with LAPS

Three species of solution with pH of 3.32, 7.04 and 9.45 were used as the solutions to be measured. The frequency of LED was set at 3 kHz. The normalized photocurrent response *I–V* curves were shown in Fig. 4(a). From the figure we can see that the transition part of the LAPS curve had a good linearity. Fig. 4(b) shows the relationship between the pH and the corresponding three curves' bias voltages where the corresponding normalized photocurrent was 0.4. It is obvious that the voltage had a linear relationship with the pH. The sensitivity (slope) is 53.9 mV/pH with a linearity coefficient of $R^2 = 0.9998$ in the range of pH 4–9. For cell analysis, the cell culture medium was always kept at about 7.4 for cell living. When used for long-time monitoring, the bias voltage was fixed at the working point. The pH change could then be obtained by monitoring change of the photocurrent.

As mentioned, *I–V* curve in the working region (from V_{min} to V_{max}) is almost linear, with photocurrent from near zero to I_{max}. The value of $(V_{max} - V_{min})$ is about 350 mV. Bias voltage is fixed at $V_0 = (V_{max} + V_{min})/2$ during detection, so the corresponding I_0 is $I_{max}/2$. The pH sensitivity is 53.9 mV/pH.

$$\Delta V = 53.9\,\text{mV} \times \Delta\text{pH} \tag{1}$$

Thus, when the bias voltage shifts from V_0 to V' ($\Delta V = V' - V_0$) due to the pH change, the photocurrent shifts from I_0 to I'.

$$I' - I_0 = I_{max} \times \frac{V' - V_0}{350\,\text{mV}} = I_0 \times \frac{\Delta V}{175\,\text{mV}} \tag{2}$$

From Eqs. (1) and (2), the relationship between pH change and photocurrent change can be determined.

$$\Delta\text{pH} = \frac{175\,\text{mV}}{53.9\,\text{mV}} \times \frac{\Delta I}{I_0} \approx 3.25 \times \frac{\Delta I}{I_0} \tag{3}$$

Therefore, a difference of 1% in photocurrent corresponds to 0.0325 in pH units.

Cell experiments were performed to detect the acidification. After the cardiac myocytes were cultured on the areas with small wells, the chamber was sealed and filled with electrolyte solution mentioned before. The volume of the testing chamber was about 100 μl. The results are shown in Fig. 4(c). First, the flow of solution was turned off for about 5 min to accumulate the H^+. Then the flow was turned on and the output rose back. When the output returned to the origin level, the flow was turned off again and the second cycle began. As we can see, when the flow was turned off, the output started to drop after several seconds. This suggests that the pH of the electrolyte solution was dropping, and the metabolism of cells acidified the solution. The output rose back quickly to the origin level after the flow was turned on. At last, electrolyte solution containing acetylcholine at the concentration of 100 mg/ml was pumped in to the chamber as the inhibitor, and the flow was turned off. After the electrolyte solution containing acetylcholine was added, the output did not drop even with the flow off, showing the cells slowed or stopped acidification, which means the cells were probably killed.

3.3. Extracellular potential signal detection

Extracellular potential detection was performed. Cardiac myocytes were used as the source of extracellular potential detection. The focused laser, 10 μm in diameter, was used for addressing

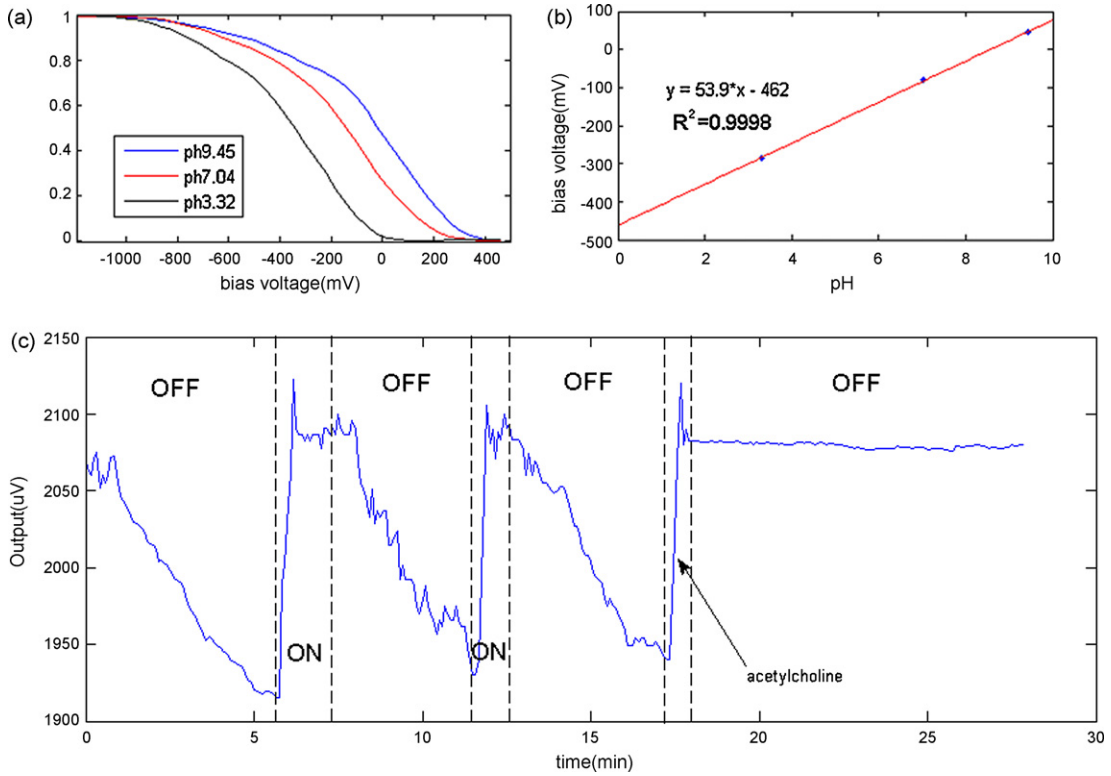

Fig. 4. (a) Normalized *I–V* curves with corresponding pH of 3.32, 7.04 and 9.45. (b) Relationship between the pH and the bias voltages corresponding to the normalized photocurrent of 0.4. (c) Acidification detection with flow switched on and off.

a cluster of cells. Adrenaline with concentration of 10 μg/ml was taken as stimulant, while acetylcholine of 10 μg/ml was taken as inhibitor.

Cells were taken from the rat's ventricle. Inoculation and culturing on LAPS array were carried out under rigorously controlled condition. After 2 days in culture, the experiment was carried out. The integration time of the lock-in amplifier was set to be at 3 ms and pass band was at 10 kHz ± 53 Hz. The bias voltage was fixed in the middle region, no obvious spike was recorded. As shown in Fig. 5(a), this line could be considered to be the baseline. The noise level is about 100 μV_{p-p} at the output. Adrenaline was then added to the testing chamber. Typical signals were recorded after about 2 min, shown in Fig. 5(b). As we can see, after stimulant was added, large spikes with amplitude of about 400 μV at the output were recorded. Besides, when the bias voltage was fixed in the saturated region, no such spikes were observed, which indicated that those spikes were not caused by mechanical beating of cardiac myocytes (Parak et al., 2000). After acetylcholine was added as the inhibitor (Belardinelli and Isenberg, 1983; Hartzell and Fischmeister, 1987), the photocurrent fell back to the noise level, showing no obvious spikes, as shown in Fig. 5(c).

It has been demonstrated that the different extracellular signal shapes are related to different ion current densities between cell layer and electronic device surface. It is therefore possible to distinguish the corresponding ion channel activity in the presence of inhibitor or excitant. In fully developed cultured cardiac cells, the action potential is generated by the sodium, calcium, and potassium currents across the cell membrane. The initial event is the inward sodium current, triggering a fast-rising phase of the action potential. The calcium current carries the plateau phase of the action potential and the outward potassium current repolarizes the cell.

A more detailed view of typical recording of cardiac myocytes is shown in Fig. 6.

Extracellular potential signals with sharp peaks in the rising phase were recorded (Fig. 6(I)). The positive peak lasts for between 20 and 30 ms, with an amplitude of about 0.25 mV at output.

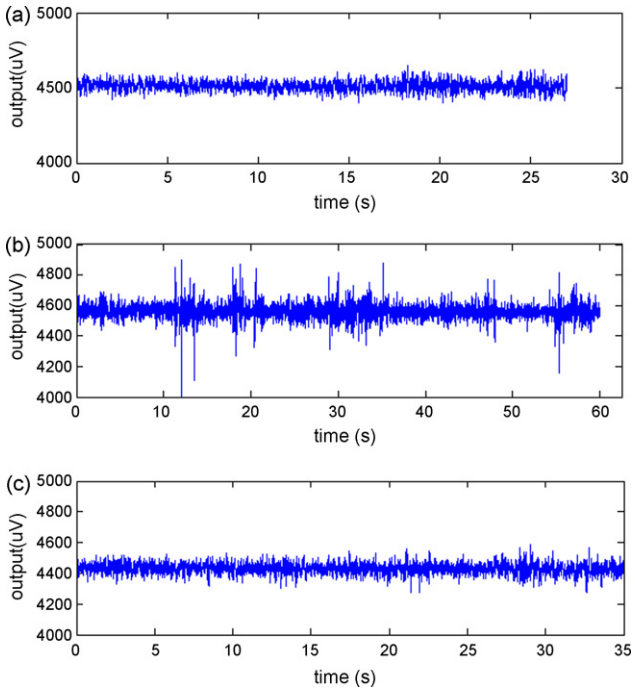

Fig. 5. Results of extracellular potential detection. (a) Baseline detected before the adrenaline was added. (b) Spikes detected after the adrenaline was added. (c) Output of the sensor after acetylcholine was added.

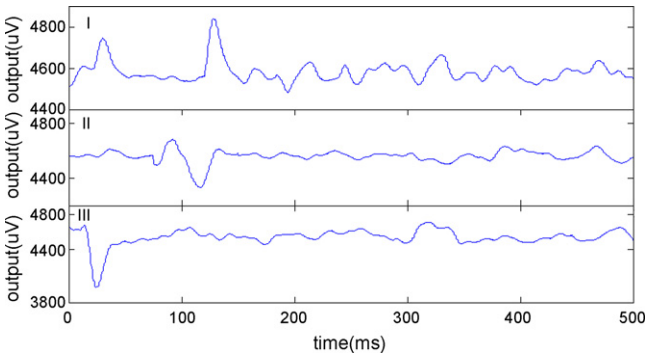

Fig. 6. More detailed view of spikes from Fig. 5(b). Extracellular recordings with a sharp peak in the rising phase of the AP ("A-type", trace I); a sharp positive followed by a negative peak ("D1-type", trace II); the sharp peaks at the beginning of the AP are followed by a second part lasting much longer ("D2-type", trace III).

According to the five classification as Sprossler mentioned for the extracellular action potential detected by FET (Sprössler et al., 1999), "A-type" has similar change trends. However, the duration of this spike was longer.

Fig. 6(II) shows another type of extracellular signals we recorded with LAPS. The overall duration of this type was about 50 ms. The sharp rise in the peak at the beginning of the AP represents about 10–50% of amplitude of the overall signal, which is about 0.12 mV at the output. The sharp rise lasts for about 20–30 ms. The duration of the second part of the peak (the negative part) is about 20–30 ms with an amplitude of about 0.25 mV. This signal was similar to the "D1-type". However, again, the duration of this spike was much longer.

Fig. 6(III) shows extracellular signals that we recorded the least. A sharp rise in the extracellular signals appears at the beginning with an amplitude of about 0.05 mV. The second part of the signal starts with a negative peak similar to the one described in Fig. 6(II). After a long recovery, a second part followed and lasted much longer for about 60 ms. The overall duration of the second part of this type of extracellular signals was about 90 ms. The amplitude of this spike is about 0.5 mV and the "D2-type" is most similar to this signal.

As we can see, these three types of extracellular potential signals detected with LAPS array showed similar trends to those recorded by FET. However, the duration of the spikes is different. This might be caused for two reasons. First, LAPS and FET are different devices. Equivalent circuit model of LAPS and FET are not exactly the same. Thus recordings by these two devices may differ from each other greatly. To solve this, much more work should be done. Second, stimulant was added, which may affect the potential signals of the cells.

We control seriously the detection environment to exclude interferes, such as signals generated by mechanical beating of cells. Thus, it is therefore reasonable to conclude primarily that the dramatically obvious signals detected are the extracellular potential signals of the cardiac myocytes under adrenaline at a concentration of 10 μg/ml.

4. Conclusion

A novel multifunctional integrated cell-based biosensor was designed to realize parallel detection of cell acidification and extracellular potential change. The living cardiac myocytes was involved as the source and the LAPS array worked as the sensor. Noise level was brought down by minimize the effective area of the testing sites and parallel detection was realized employing both lock-in amplifier and FFT technique for data sampling and demodulation. Experiment results showed that this LAPS array can reliably detect

acidification of cells as well as extracellular potential signals. However, to validate the species of extracellular potential signals, more experiments should be carried out.

This cell-based biosensor can be useful for sensor integration and multifunctional detection. Future work will be focused on planting different ion sensitive membranes on the LAPS array to simultaneously detect several different metabolic substances to evaluate the effect of drugs to the cells. This LAPS array can possibly be a platform of rigorous drug screening.

Acknowledgements

This work was supported by the National Natural Science Foundation of China (grant nos. 30570492 and 30700167), the key project from National Natural Science Foundation of China (grant no. 30627002), the Natural Science Foundation of Zhejiang Province of China (grant no. R205505).

References

Adami, M., Sartore, M., Nicolini, C., 1995. Biosens. Bioelectron. 10, 155–167.
Belardinelli, L., Isenberg, G., 1983. Am. J. Physiol. Heart Circ. Physiol. 244, H734–H737.
Bousse, L., 1982. Dissertation of Ph.D., Twente University of Technology, Enschede.
Cai, H., Xu, Y., LIU, Q.J., 2007. Chin. J. Sens. Actuators 01 (20), 58–63.
Connolly, P., Clark, P., Curtis, A.S.G., 1990. Biosens. Bioelectron. 5, 223–234.
Denyer, M.C.T., Riehle, M., Britland, S.T., 1998. Med. Biol. Eng. Comput. 36, 638–644.
Fromherz, P., 2002. Chem. Phys. 3, 276–284.
George, M., Parak, W.J., Gaub, H.E., 2000. Sens. Actuators B 69, 266–275.
Hafner, F., 2000. Biosens. Bioelectron. 15, 149–158.
Hafeman, D.G., Parce, J.W., McConnel, H.M., 1988. Science 240, 1182–1185.
Hamill, O.P., Marty, A., Neher, E., Sakmann, B., Sigworth, F.J., 1981. Pflügers Arch: Eur. J. Physiol. 391, 85–100.
Hartzell, H.C., Fischmeister, R., 1987. Mol. Pharmacol. 32 (5), 639–645.
Ismail, A.B.M., Yoshinobu, T., Iwasaki, H., 2003. Biosens. Bioelectron. 18, 1509–1514.
Men, H., Zhou, S.F., Li, Y., 2005. Sens. Actuators B 110, 350–357.
Parak, W.J., George, M., Domke, J., 2000. IEEE Trans. Biomed. Eng. 47 (8), 1106–1113.
Parak, W.J., Hofmann, U.G., Gaub, H.E., 1997. Sens. Actuators A 63, 47–57.
Shimizu, M., Kanai, Y., Uchida, H., 1994. Sens. Actuators B 20, 187–192.
Siu, W.M., Cobbold, R.S.C., 1979. IEEE Trans. Electron Dev. 26, 1805–1815.
Sprössler, C., Denyer, M., Offenhäusser, A., 1998. Biosens. Bioelectron. 13, 613–618.
Sprössler, C., Denyer, M., Britland, S., 1999. Phys. Rev. E 60, 2171–2176.
Wang, P., Xu, G.X., Qin, L.F., 2005. Sens. Actuators B: Chem. 108, 576–584.
Wolf, B., Brischwein, M., Baumann, W., 1998. Biosens. Bioelectron. 13 (5), 501–509.
Wu, Y.C., Wang, P., Ye, X.S., 2001. Sens. Actuators B 80, 215–221.
Xu, G.X., Ye, X.s., Qin, L.F., 2005. Biosens. Bioelectron. 20, 1757–1763.
Xu, Y., Cai, H., Liu, Q.J., 2006. Rare Met. Mater. Eng. 35, 51–54.